CHEMISTRY
A EUROPEAN JOURNAL

DOI: 10.1002/chem.200601428

Exhaustive Analysis of Frontal Copolymerization of Functionalized Monovinyl and Divinyl Monomers

Narahari S. Pujari,[a] Satish R. Inamdar,[b] Jalindar D. Ambekar,[c] B. D. Kulkarni,[a] and Surendra Ponrathnam*[a]

Abstract: A series of copolymers of 2-hydroxyethyl methacrylate (HEMA)/glycidyl methacrylate (GMA) and ethylene dimethacrylate (EGDM) were synthesized by frontal polymerization (FP). This study was conducted to investigate the effect of crosslink density, type and concentration of initiator, the use of a complex initiator system, porogen, and diluent on the most relevant parameters of FP, such as sustainability of the front, temperature profile, front velocity, and yield. The products were also characterized for intruded pore volume, pore-size distribution, epoxy-functionality number, and surface morphology. Higher crosslink densities (CLDs) and initiator concentration produced higher front velocities, whereas no trend in front temperature was noted. A complex initiation system was effective in stabilizing and increasing the polymerization yield. Relative to suspension polymerization (SP), FP products synthesized without a solvent were microporous, whereas micro-to-macroporous products were obtained in the presence of a solvent (for HEMA–EGDM polymers). We also present, explain, and discuss the exotic patterns observed under a microscope. We observed two basic types of spatial patterns, namely, planar and nonplanar patterns. The type of planar pattern observed under scanning electron microscopy (SEM) has a spatial impulse that appears as a loop followed by regular periodic motion in the radial and axial directions. This behavior gives rise to a repeating pattern that is a few microns thick. Also, nonplanar patterns, namely, layered concentric rings and winding staircase patterns, were observed under SEM.

Keywords: copolymerization · patterns · polymers · porosity

Introduction

Frontal polymerization (FP) is a technique in which the monomer converts into the polymer through a localized region that propagates in the form of a moving front as a result of the interplay between thermal conveyance and temperature-dependent reaction rates. After the first observation of this technique,[1] Pojman et al. carried out an extensive study of the macrokinetics and dynamics of FP in which properties such as front velocity, conversion, and the effect of different system components were studied.[2–6] Over the last couple of years, the technique has been applied to diverse fields such as polymer nanocomposites,[7] superabsorbant polymers,[8,9] functionalized crosslinked copolymer networks,[10,11] copolymers,[12,13] and the consolidation of stone.[14]

In the case of mono- and multivinyl systems (crosslinking agent), a sharp front propagates through the reaction media, as polymerization and crosslinking occur simultaneously. The mechanism of this process is similar to that in the conventional free-radical polymerization systems. Initially, the monomer(s) is placed in a test tube together with a thermally unstable initiator. After applying a heat source, the initiator decomposes and radicals form and begin to combine with the monomers, thus forming new radicals. The new radicals then bond with other monomers, thereby causing chains to grow. Eventually each chain combines with a second radical and terminates the growth and produces a polymeric structure. Crosslinking in FP yields rigid thermosets with novel microstructures and morphologies capable of withstanding high temperatures.[15]

[a] N. S. Pujari, Dr. B. D. Kulkarni, Dr. S. Ponrathnam
Polymer Science & Engineering Group
Chemical Engineering and Process Development Division
National Chemical Laboratory
Pashan Road, Pune-411008 (India)
E-mail: s.ponrathnam@ncl.res.in

[b] Dr. S. R. Inamdar
Department of Chemical Engineering
Vishwakarma Institute of Technology
Upper Indiara Nagar, Bibwewadi, Pune-411037 (India)

[c] J. D. Ambekar
Center for Materials for Electronic Technology
Pashan Road, Pune-411008 (India)

Nagy et al.[16] and Szalay et al.[17] prepared filled materials and composites by FP from mixtures of triethylene dimethacrylate and acrylamide comonomer using different fillers. Washington and Steinbock[18] and recently Yan et al.[8,9] reported the formation of hydrogels, and Fiori et al.[19] studied the effect of the crosslinker in the curing of unsaturated polyester resins. Similarly, interpenetrating networks and functionalized networks were reported by Pojman et al.[20] and Pujari et al.,[10,11] respectively. Likewise, the effect of convection on the propagating front was analyzed by Bowden et al.[21] on a model copolymerization reaction of acrylamide *N*,*N*-methylenebisacrylamide in dimethyl sulfoxide (DMSO). Masere et al.[22] observed a periodic doubling bifurcation sequence on varying the crosslinker feed ratio, and a magnetic resonance imaging (MRI) technique was used by Manz et al.[23] to analyze the spin modes in the copolymerization of 1,6-hexane diacrylate and pentaerythritol tetraacrylate. Recently, Binici et al.[24] reported spherical front propagation in a 1,6-hexanediol diacrylate system. A multivinyl monomer is important in FP as it decreases the nucleation of the bubbles and the Taylor and double-diffusive instabilities.[15]

FP resembles self-propagating high-temperature synthesis (SHS) in that both techniques involve a variety of intricate physiochemical processes, such as melting, diffusion of heat, and the confinement of the reaction in a localized region. The reaction mechanism is not well understood. The reaction is triggered at one end of the reactor by ignition, and polymerization/SHS self-propagates as a front.[25] One of the features of FP, also akin to SHS processes, is the presence of various instabilities. In the simplest steady state, all of the wave points will move with a constant and ideal velocity. The thermal feedback between the chemical kinetics and the heat diffusion results in a sustainable traveling wave. The uniformly propagating wave will become unstable under certain parametric regimes. The dynamics have been studied numerically and analytically in SHS.[26–31] It has been established that heat conduction and diffusion processes determine the structure of the wave front. When there is a competition between heat production in the reaction zone and heat diffusion from the reaction zone to the cold reactants, the front may become thermally unstable. The front absorbs the excess energy into itself and thereby enters a generally unstable state. Experimentally, for the first time, the loss of stability was observed for the anion-activated polymerization of ε-caprolactum in FP.[32] A subsequent study was carried out by Pojman et al. in 1995,[33] and since then a number of authors have reported the presence of various instabilities and have put forth stability analyses.[22,25,33–41] To date, the four types of instabilities that have been identified in FP are 1) thermal, 2) convective, 3) fingering (Rayleigh–Taylor), and 4) hydrodynamic instability.

Herein, for the first time, we report exotic patterns observable under a microscope. When the thermal diffusion does not spread across adjacent layers of a liquid mixture of monomer and initiator, planar wave propagation occurs in the axial direction. During this axial motion, a spiral core forms radially, and before this core descends down towards the bottom of the reactor, a spiral wave propagates to reach the reactor-tube boundary. Inamdar et al.[42] first showed these patterns formed during the FP of 2-hydroxyethyl methacrylate. They demonstrated that the motion gives rise to a characteristic spatial pattern as a result of nonlinear coupling between thermal diffusion and reaction kinetics. Pattern formation in the radial direction was not visible to the naked eye and was observed only with scanning electron microscopy (SEM). This pattern was regular and the microstructure and morphology of the solidified polymer prepared in the reactor tube was preserved.

Beaded poly(glycidyl methacrylate–*co*-ethylene dimethacrylate) (poly(GMA–EGDM)) and poly(2-hydroxyethyl methacrylate–*co*-ethylene dimethacrylate) (poly(HEMA–EGDM)) have a reactive epoxide ring and a hydroxy group in the side chain, respectively, which are useful in the design of a whole range of compounds with various functional groups.[43] The optimal morphological porous structure of these crosslinked network copolymers has been demonstrated for application as catalysts, chromatographic materials, separation and adsorbent media, immobilization matrices for enzymes, and agents in clinical fields.[44,45] We have previously presented preliminary results of the synthesis of functionalized crosslinked copolymer networks of 2-hydroxyethyl methacrylate (HEMA)/glycidyl methacrylate (GMA) and ethylene dimethacrylate (EGDM) by FP and compared these networks with those formed by suspension polymerization (SP).[10,11] It was shown that FP leads to porosity in the matrix, even in the absence of a porogen, as a result of the gases evolved (decomposition of azobisisobutyronitrile (AIBN)) and the osmotic pressure of the monomers. High temperature in FP led to the formation of narrow pore size and narrow pore-size distribution.

Herein, a comprehensive analysis of the FP of monovinyl-functionalized monomers HEMA and GMA with the divinyl monomer EGDM is reported. In first part of this study, the effect of the type and concentration of the initiators and solvents as well as complex initiation and the mode of FP (descending and ascending) system on the sustainability and shape of the front, front velocity, front temperature, and yield (%) are investigated. The polymers are exhaustively characterized in terms of their micro/macroporosity in the matrix, gel formation, and surface morphology and compared with identical compositions prepared by SP. Later, we present a detailed account of the experimental observations using SEM images, which show the formation of spinning modes in FP. The propagation of spin modes gives rise to layered patterns in the solidified polymer material. The physicochemical phenomenon of the pattern formation is also discussed.

Results and Discussion

Free-radical frontal copolymerization between a mono- and multivinyl comonomer forms a thermoset. In the present

system, EGDM is the difunctional monomer. The reactivity ratios r_1 and r_2 for the GMA and EGDM systems are 0.98 and 1.00, respectively,[44] whereas in the HEMA and EGDM systems r_1 and r_2 are 0.84($\pm$0.20) and 6.2, respectively.[46] When r_1 and r_2 are close to unity and the front temperature of polymerization is quite high, the composition of the copolymer is expected to mirror the monomer feed ratios. For the copolymerization of HEMA with EGDMA, $r_2 \gg r_1$, which means that both types of radicals react preferentially with EGDMA. There is a tendency for successive homopolymerization of the two monomers; therefore, a heterogeneous network is expected to form. During FP, the situation is rather complicated and the reactivity ratio concept may get violated because of a high front temperature and rapid reaction rates. As a result of the high temperature and the presence of oxygen in the system, side reactions and premature termination are expected to take place, thus leading to a complex crosslinked structure. The conditions for the preparation of heterogeneously crosslinked copolymers from the GMA–EGDM and HEMA–EGDM systems are shown in Tables 1 and 3.

Front shape, propagation, and bubbles: In all the reactions, large and small bubbles were generated at the beginning and the front was uneven and propagated randomly (Figure 1). The bubble layer can act as an insulating layer for heat transfer and causes a slow pulsation of the moving front. The front attains stability after such an uneven propagation for 2–3 cm. This stability depends on the amount of crosslinker, initiator type, and initiator concentration. The diffusion of heat through the bubble to the adjacent layer is critical. Bubbles are formed as a result of the liberation of gaseous products due to initiator decomposition, monomer vapors, and the presence of traces of moisture in the monomer solution. As the bubble grows, it pushes the monomer out of its path. At the front temperature, there is a rolling motion of low-viscosity polymer and monomer. The monomer rapidly heats up as it reacts, thereby increasing the volume of the bubble. Because bubbles are descending, the monomer can only swell and push up.[47] Competition now ensues between the descending bubbles and expanding monomer. In this process, the bubbles generally find their way down and the monomer rises, whereupon it polymerizes, thus triggering a repetition of this process. If convection is higher and the bubbles are in a large excess, heat is removed in the process and the front ceases. In some examples, the polymerization front was forced upward as a result of convection and pressure generated by the monomer(s). This behavior happens when thermal expansion exceeds the isothermal contraction, thus creating a gap between the polymer and monomer liquid layers, which results in a complete cessation of the polymerization process (Figure 2). This behavior was predominant in the presence of a solvent (e.g., G20–43). We also encountered velocity lag, for which an additional heat impetus for 2–5 s (e.g., H3 and G3) was needed.

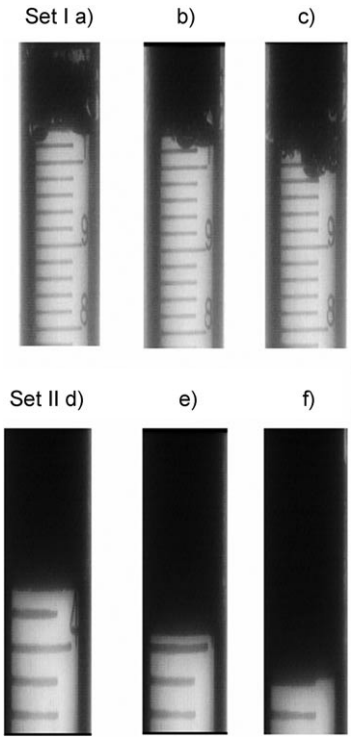

Figure 1. Snapshots of front propagation in a complex initiation system (GMA—EGDM: CLD: 100 mol%; AIBN+DCP: 2 mol%). a–c) Front propagation is uneven and in the form of bubbles; d–f) front is stabilized and propagation is even without bubbles. The images were taken by high-speed CCD camera (Motionpro) at a speed of 50 frames s^{-1}; the above montages are the images obtained after every 5 s in each set.

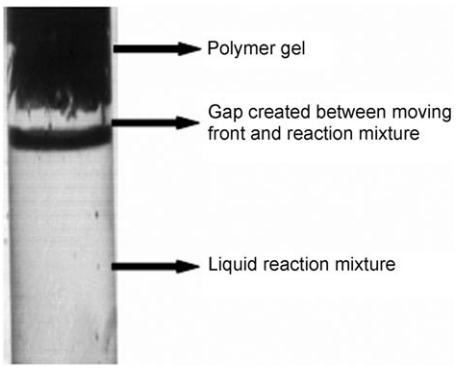

Figure 2. The front was extinguished as a result of the gap created between the monomer and propagating polymerization front (G27; reactor size: 12×125 mm; BPO: 4 mol%; EGDM: 100 mol% CLD; monomer/porogen: 1:0.4, v/v).

Initiator effects: The front velocity is related to the initiator concentration and crosslink density (CLD).[3,4] Copolymerization reactions were evaluated at concentrations of 2 and 4 mol% for AIBN and BPO (Table 1; H1–H20 and G1–G20) as well as with dicumyl peroxide (DCP; not shown in Table 1). For AIBN and BPO, clear fronts were observed in both the HEMA–EHDM and GMA–EGDM systems at concentrations of 2 and 4 mol% (sometimes an additional

Table 1. Experimental variables used for the copolymerization of the HEMA–EGDM and GMA—EGDM systems: Effect of variation of the initiator type and concentration.[a]

Code no.	CLD [mol %][b]	AIBN [mol %]	BPO [mol %]	Code no.
H1	25	–	2	G1
H2	50	–	2	G2
H3	100	–	2	G3
H4	200	–	2	G4
H5	400	–	2	G5
H6	25	–	4	G6
H7	50	–	4	G7
H8	100	–	4	G8
H9	200	–	4	G9
H10	400	–	4	G10
H11	25	2	–	G11
H12	50	2	–	G12
H13	100	2	–	G13
H14	200	2	–	G14
H15	400	2	–	G15
H16	25	4	–	G16
H17	50	4	–	G17
H18	100	4	–	G18
H19	200	4	–	G19
H20	400	4	–	G20

[a] H1–20 and G1–20: Frontal copolymerization reactions using the HEMA–EGDM and GMA—EGDM systems, respectively. For FP: heating time: ≈60 s; total reactant volume: 8.2 mL. Identical compositions were synthesized by SP (SP): *T*: 70 °C, stirring speed: 300 rpm, reaction time: 3 h. [b] CLD: (mol of EGDM)/(mol of HEMA/GMA + mol of EGDM) × 100.

impetus of 5–10 s had to be given at lower CLDs), thus leading to the formation of the polymeric product, which took the shape of the reactor (cylindrical). No double-diffusive instabilities were observed. Table 2 summarizes the details of the front velocity, temperature, and yield (%). No specific trend was observed at low initiator concentration for the HEMA–EGDM system. Figure 3 is a representative depiction of the front velocity ($cm\,min^{-1}$) as a function of the

Table 2. Front velocity (FV), front temperature (FT), and yield of the reactions performed as in Table 1.

Code no.	FV [$cm\,min^{-1}$][a]	FT [°C]	Yield [%][b]	Code no.	FV [$cm\,min^{-1}$][a]	FT [°C]	Yield [%][b]
H1	1.37	175	85.81	G1	0.71	177	86.22
H2	1.10	182	92.71	G2	0.87	187	88.23
H3	1.19	185	94.54	G3	0.94	190	91.25
H4	1.09	185	89.38	G4	0.95	199	90.35
H5	1.42	187	92.26	G5	1.01	198	92.55
H6	0.89	192	84.12	G6	0.76	186	86.70
H7	0.95	196	90.21	G7	0.92	196	85.60
H8	1.06	198	92.45	G8	0.97	183	83.60
H9	1.16	200	91.12	G9	1.03	187	89.41
H10	1.2	203	94.45	G10	1.11	191	95.10
H11	0.87	175	89.12	G11	0.81	189	80.32
H12	0.95	169	87.35	G12	0.86	197	80.67
H13	0.83	172	96.02	G13	0.88	194	81.23
H14	0.85	162	86.10	G14	0.92	179	83.88
H15	0.87	158	97.40	G15	0.94	181	81.16
H16	0.82	181	85.56	G16	0.83	184	82.10
H17	0.92	190	86.12	G17	0.88	187	79.24
H18	0.93	193	94.51	G18	0.9	191	87.10
H19	1.08	198	84.94	G19	0.97	167	92.70
H20	1.20	198	95.53	G20	1.22	178	86.25

[a] FV values were measured with a precision of ±0.10. [b] Percent yield of the polymer.

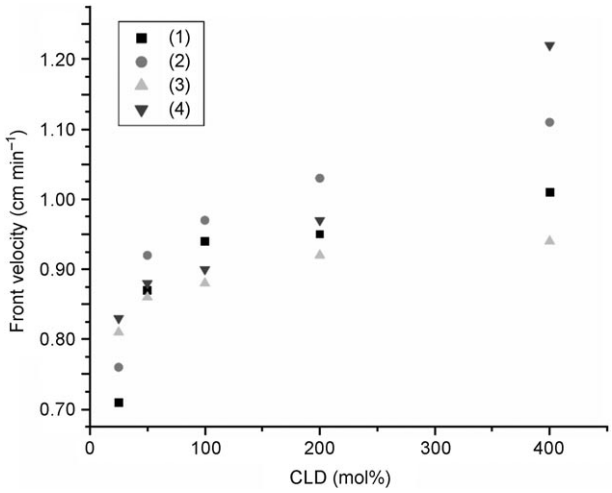

Figure 3. Representative graph of front velocity ($cm\,min^{-1}$) versus CLD (mol %) of poly(GMA–EGDM). Poly(GMA–EGDM) was synthesized using 1) 2 mol % BPO; 2) 4 mol % BPO; 3) 2 mol % AIBN, and 4) 4 mol % AIBN.

CLD at the two concentrations (2 and 4 mol %) of AIBN and BPO in the GMA–EGDM system. It is clear that front velocities are higher at an initiator concentration of 4 mol % for all monomer feed compositions (CLD; mol %). The increase in radical concentration increases the rate of heat generation and thus the velocity of FP. It was also seen that the front velocity increases with the CLD. With a high CLD, the rate of termination decreases, which in turn increases the activation energy of the reaction. In other words, multifunctional vinyl compounds react faster at room temperature than monovinyl monomers.[22] A relative increase in divinyl monomer concentration (EGDM) leads to more inter- and intramolecular crosslinking reactions. A comparison of the two initiators indicates that AIBN produces slightly faster fronts than BPO.

The results with DCP, however, were different. DCP is a thermally stable initiator (activation energy: 147.42 $kJ\,mol^{-1}$[48]). Front sustainability (i.e., the activation energy of the polymerization front) depends upon the decomposition activation energy of the initiator. At low DCP concentration (2 mol %), as a result of its high decomposition activation energy, a front propagation was initiated but ceased after propagating for a short distance (50–80 % of the column length) for both copolymerization systems (GMA–EGDM and HEMA–EGDM). The radiational and convective heat loss could bring the front temperature below that required to sustain the front. At a concentration of 4 mol %, a sharp transparent front propagation was observed. In both sets, at CLDs of 25 and 50 mol %, a long trail of bubbles could be seen during polymerization or on the specimen after polymerization (Figure 4). At a CLD of

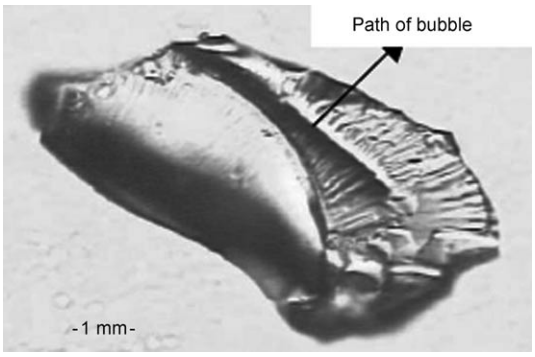

Figure 4. A path of a bubble observed in a DCP-initiated poly(GMA–EGDM) system (DCP: 4 mol %; CLD: 50 mol %).

100 mol %, a transparent front propagation was observed. However, the front could not be sustained at higher CLDs perhaps due to the increase in activation energy with the increasing CLD needed to sustain the front. The greater the stability of the initiator, the higher the overall energy of activation of the front, the slower the front velocity. Therefore, in both sets, the front velocities were low and in the range 0.4–0.6 cm min^{-1}. With AIBN, a velocity lag was observed at higher CLDs as a result of a density gradient between the polymer and monomer reaction mixture. This result was circumvented by adding diluents, such as silica gel, to increase the viscosity of the medium or by giving an additional heat impetus for 5 s.

The front temperature is dictated by a combination of factors, such as the enthalpy of the reaction, the heat capacity of the product, and heat lost to the surroundings. Table 2 shows that the front temperature varied within (±10) °C for all the polymerization processes of identical compositions. Also, the front temperature was generally high at higher CLDs (100, 200, and 400 mol % (180±10) °C) for all compositions. The front temperature was lower with AIBN at a concentration of 2 mol % in the HEMA–EGDM system. As a general trend, the data reveal that the front temperature oscillates with monomer feed composition, with maxima in the CLD range 50—100 mol %, and then a minima at a CLD of 200 mol %, followed by a gradual increase until a CLD of 400 mol %, at initiator concentrations of both 2 and 4 mol %. Temperature drift, however, is not very high and is in the range at which thermal fluctuations exceed the variations in the temperature. With DCP, as expected, in the reactions which ceased, the temperature was lower (153± 5) °C; otherwise, it was (180±3) °C.

Initially, the problem in FP was the lower conversions because of the high front temperature, which is responsible for rapid initiator decomposition or "burning out". Gel formation in FP is known to flatten front curvature, prevent instabilities, and increase yield.[3] In the system studied herein, we observed higher conversions relative to those previously reported;[51] however, there was no trend. Generally, maximum conversions were observed at higher CLDs (Table 2). This behavior may be attributed to the fact that increasing the concentration of EGDM with two reactive double bonds decreases transfer reactions.

Solvent effects: High-boiling-point solvents are needed to produce a propagating front; at the same time the temperature also should be high enough to produce a sufficiently rapid decomposition of the free-radical initiator. A front can sustain itself only when the volumetric rate of heat generated exceeds the volumetric rate of heat loss incurred by heat dissipation as a result of solvent and convective losses. Whereas the rate of the conduction heat loss increases linearly with temperature, the free-radical-initiator decomposition is a high activation-energy process whose rate increases much more rapidly than linearly with temperature. Thus, as the temperature decreases, the ratio of heat loss to heat generation increases, thus eventually leading to extinction of the front if the temperature is too low. We conducted our experiments with dimethyl sulfoxide (DMSO), paraffin, dichloroethane, dodocane, cyclohexanol, cyclohexane, and 2-ethoxyethyl acetate (EEA) in monomer/solvent ratios of 1:0.4 and 1:0.8 (v/v), with the initiator concentration (AIBN and BPO) at 2 and 4 mol % in both sets. Amongst all the solvents, the front could be sustained only with EEA in the HEMA–EGDM system (Table 3). In presence of low-boiling-point solvents, the front could not start and only the boiling of the monomer mixture was observed, and in others, the front extinguished at lower conversions (10–30 % of the column length).

Table 3. Experimental variables used for copolymerization of HEMA–EGDM and GMA–EGDM: Effect of the variation of solvent volume.[a]

Code no.	CLD [mol %]	AIBN [mol %]	BPO [mol %]	EEA [mL]	Code no.
H21	25	–	2	2.36	G21
H22	400	–	2	2.36	G22
H23	25	2	–	2.36	G23
H24	400	2	–	2.36	G24
H25	25	–	4	2.36	G25
H26	50	–	4	2.36	G26
H27	100	–	4	2.36	G27
H28	200	–	4	2.36	G28
H29	400	–	4	2.36	G29
H30	25	–	4	3.67	G30
H31	50	–	4	3.67	G31
H32	100	–	4	3.67	G32
H33	200	–	4	3.67	G33
H34	400	–	4	3.67	G34
H35	25	4	–	2.36	G35
H36	50	4	–	2.36	G36
H37	100	4	–	2.36	G37
H38	200	4	–	2.36	G38
H39	400	4	–	2.36	G39
H40	25	4	–	3.67	G40
H41	50	4	–	3.67	G41
H43	100	4	–	3.67	G42
H43	200	4	–	3.67	G43
H44	400	4	–	3.67	G44

[a] For FP: heating time: ≈60 s; the total reactant volume: 8.2 mL. Identical compositions of the HEMA–EGDM system (H25-H44) were synthesized by SP (SP): *T*: 70 °C, stirring speed: 300 rpm, reaction time: 3 h.

Porogens (synonym used for solvent) are solvating or non-solvating inert reagents used to generate a "tailor-made" porous structure in crosslinked polymer networks synthesized by SP.[43] In the GMA–EGDM system, the polymer formed immediately after the initial ignition and the front propagation was started. At all compositions, although the front propagation was initiated, it extinguished after propagating approximately 50% of the column length. The porogen dissipates the threshold heat required to sustain the front. The front temperature was significantly low (130–140°C). We then performed a few reactions using a diluent, which is an inert material that acts as a filler and is added to inhibit buoyancy-induced convection in the solutions.[3] FP carried out using silica gel as the diluent achieved completion only at a CLD of 400 mol%.

In HEMA–EGDM polymerization, however, the front could be sustained in EEA at an initiator concentration of 4 mol%. At 2 mol% of AIBN and BPO, the front ceased after the initial burst and little propagation (Table 3, H21–H24). Porogen type has marginal influence on the rate of polymerization in SP, but it has a strongly favorable effect in FP. Porogens such as cyclohexane and DMSO quenched the front as a result of extensive heat loss, whereas EEA sustained the front with both AIBN and BPO. The main rational for EEA sustaining the front in the HEMA–EGDM system but not the GMA–EGDM system is the slow phase separation of EEA in HEMA–EGDM as a result of solvation. In the HEMA–EGDM system, there was a marked difference in front velocities and temperatures with AIBN and BPO. BPO produced higher rates of polymerization (Table 4). In both systems, front velocity and temperature increased with CLD. The rate of polymerization in the monomer/porogen system was also found to be dependent on the CLD. With AIBN, bulk polymerization competed with FP at a higher volume of porogen (1:0.8, v/v; Table 3, H40–H44). AIBN, which has a low activation energy, decomposes rapidly and the porogen transferred the heat to the subsequent layers, thus causing bulk polymerization to occur. However, no bulk polymerization was observed with BPO, and the reactions were completed by true FP. All the reactions with DCP ceased as a result of extensive heat loss.

Table 4. Front velocity, front temperature, and yield of the reactions presented in Table 2.

Code no.	FV [cm min^{-1}][a]	FT [°C]	Yield [%][b]
H21–24		no reaction	
H25	0.64	169	66.78
H26	0.68	163	75.34
H27	0.78	186	93.12
H28	0.82	189	92.44
H29	0.80	175	91.9
H30	0.75	172	67.11
H31	0.44	187	71.96
H32	0.40	181	83.66
H33	0.24	185	96.00
H34	0.20	179	96.03
H35	0.27	141	81.49
H36	0.37	147	85.86
H37	0.47	145	81.73
H38	0.74	154	95.89
H39	0.43	166	87.67
H40	0.22	86	76.21
H41	0.32	105	75.54
H42	0.26	121	80.24
H43	0.48	115	72.62
H44	0.22	122	72.98

[a] FV values were measured with a precision of ±0.10. [b] Percent yield of the polymer.

Complex initiation: High front temperature causes depletion of the initiator, which in turn lowers the conversion (%) in FP. A mixed initiation system comprising AIBN and DCP was developed based on a strategy that the lower activation-energy initiator will increase the rate of polymerization, while the higher activation-energy initiator will increase conversion.[49,50] It was indeed observed that the front was stabilized and that the yields were much higher (>96%). The nature of the front was flat after the initial uneven propagation (see Figure 1). When the reaction is triggered, AIBN, with a lower activation energy, is decomposed more rapidly, whereas DCP, with a higher activation energy, stabilizes the front. Thus, AIBN ensures moderate velocity, whereas DCP polymerizes the final traces of the unreacted monomers before the front moves, thereby ensuring a higher conversion. At a concentration of 2 mol% (without solvent), AIBN/DCP (2:1, mol/mol) generated higher front velocities in both the HEMA–EGDM and GMA—EGDM systems relative to DCP alone at a concentration of 4 mol%. Figure 5 presents the front-velocity data of the HEMA–EGDM system. Front velocities were almost constant ((0.93±0.02) cm min^{-1}, except CLD=25 mol%). The front temperature was also slightly lower (151–172°C), and, as expected, the yields were high ((97±2)%). Similarly, in the GMA–EGDM system, the front velocities were almost constant and relatively faster than that in the HEMA–EGDM system (Figure 5). The front temperatures of 160–

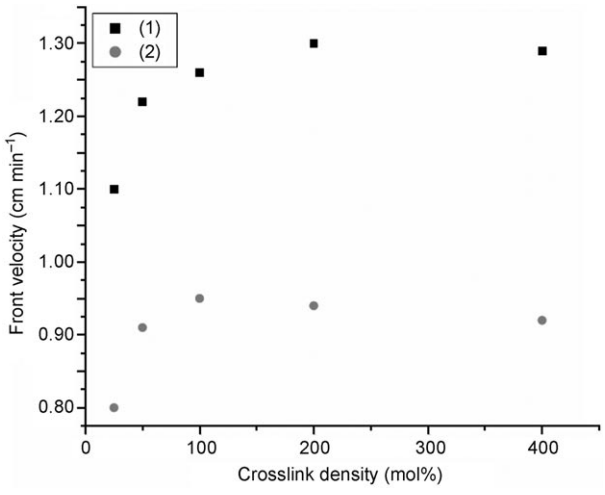

Figure 5. A graph of front velocity versus CLD for a complex initiator system (AIBN+DCP: 2 mol%): 1) poly(HEM–EGDM) and 2) poly(GMA–EGDM) systems.

180 °C and yields of (98±2) % were comparable with those in the HEMA–EGDM system.

We also conducted reactions on mixtures comprising monomer(s), mixed initiators (2 mol %), EEA (porogen), and a diluent (silica gel; 5 wt % of monomer). At a ratio of 1:0.4 for monomer/porogen (v/v), it was observed that additional heat impetus was needed for 5 s for the reaction to go to completion. The shape of the front was flat, and the products obtained were opaque. In both sets, front propagation did not go to completion at higher CLDs (200 and 400 mol %). All reactions carried out at a monomer/porogen ratio of 1:0.8 (v/v) ceased, even in presence of the diluent. The reason for this behavior is that the front temperature was not sufficient to sustain front propagation.

Ascending polymerization: To understand front-propagation behavior, we conducted selected reactions in both the HEMA–EGDM and GMA–EGDM systems with and without a solvent at CLDs of 25 and 100 mol % by giving heat impetus at the bottom of the reactor. Ascending fronts are, generally, not stable as a result of convective motions, which cause an extensive amount of dispersed heat.[5,21,51] In our methodology, when the reaction was performed without solvent, the ascending front went through in a nonplanar mode in both sets. The front propagated in the upward direction and yielded a polymer gel. The propagation was along the walls of the reactor first and was clubbing at the center. DMSO ceased descending polymerization, but ascending polymerization went to completion when performed with a monomer/DMSO ratio of 1:0.4 (v/v) in presence of a diluent (silica gel) in both sets. All the other solvents studied could not produce stable fronts.

Comparison with suspension polymerization: In our previous report, we compared front polymerization (FP) to suspension polymerization (SP) without a porogen and at a AIBN concentration of 2 mol %.[10,11] Herein, more detailed analysis and comparisons are presented. We compared the GMA–EGDM and HEMA–EGDM polymerizations at AIBN and BPO concentrations of 4 mol %. As solvents ceased the reactions in the MA–EGDM system, we only evaluated and compared the HEMA–EGDM system with the porogen EEA, at monomer/porogen ratios of 1:0.4 and 1:0.8 (v/v) with AIBN and BPO concentrations of 4 mol % (Table 3), with identical compositions prepared by using SP. All the polymers were characterized by IR spectroscopy, epoxy/hydroxy number, surface area, pore volume, porosity, solvent/nonsolvent regain, and SEM analysis.

SP is widely used to synthesize macroporous beaded polymers. Beads have an internal porosity in both the swollen and dry states. The macroporous structure results from phase separation of an inert organic solvent (porogen)[43] from the discontinuous polymerizing droplet. For the production of macroporous copolymers, a typical recipe comprises a monovinyl monomer, a divinyl monomer (crosslinker), an initiator, and an inert porogen (diluent). The decomposition of the initiator produces free radicals that initiate the polymerization and crosslinking reactions. After a certain reaction time, a three-dimensional network of infinitely large size starts to form. At this point (the gel point) the system (monomer/diluent mixture) changes from a liquid to solid-like state. Continuing the polymerization and crosslinking reactions decreases the amount of soluble reaction components. After complete conversion of the monomers into polymer, only the network and the diluent remain in the system. Crosslinked copolymers prepared by free-radical copolymerization exhibit differing pore structures and surface properties (within the pores), depending on the amount of the crosslinker and diluent present during the reaction and on the solvating power of the diluent. We have used higher CLDs of crosslinker in our system. Increasing the divinyl monomer (EGDM) content in the monomer mixture (increase in CLD (mol %)) leads to an increase in the size of the nucleus at the expense of the growing chains. The product that results from the high conversion of the monomer mixture, namely, high divinyl monomer content, is therefore a compact and rigid structure with marked network entanglement in the nuclei. In FP, there is rapid crosslinking as a result of the high front temperature. Phase separation occurs instantaneously and polymerization propagates as a phase-separated polymer front. Gel is continuously formed as the front propagates. Initiation occurs evenly throughout the layers (propagating reaction zones) and chains grow by the addition of monomer units. We conceive no drift in the final composition as the polymerization process is stoichastic in the narrow reaction zone. We believe that porosity is independent of the divinyl monomer but dependent on the solvent. When an EGDM molecule is added to a growing chain, the chain carries a pendent double bond, which may be incorporated in another growing chain. Unlike SP, there is no nuclei formation in FP. Polymer chains are less solvated. Porosity in FP is due to the gases, monomer, and solvent vapors being released during the reaction. This porosity is discontinuous in the absence of a solvent. Solvent (porogen) develops higher porosity in the matrix. As seen above, all our reactions, except that with EEA, failed. EEA is a high-boiling liquid and probably solvates the polymer chains. Therefore at the front temperature, a partial phase separation takes place, which on removal of the solvent creates the higher pore volume and porosity.

The formation of the copolymer network was confirmed by IR spectroscopy.[10,11] Epoxy/hydroxy numbers for all polymers were lower than the theoretical value, thus indicating possible intramolecular reactions, as observed in HEMA homopolymerization,[52] as a result of disproportionate termination reactions and partial opening of the epoxy ring at high temperature (front temperature) through etherification.[11] At higher CLDs, the probability of side reactions is decreased as a result of the high reactivity of the bifunctional monomer EGDM, which predominantly undergoes crosslinking reactions rather than side reactions; thus, the loss of functionalities can be considerably reduced. For example, the experimentally observed surface epoxy value of FP at a

CLD of 200 mol% was 1.79 mmol g^{-1}, which is very close to the theoretical value of 2.01 mmol g^{-1}. Instead, the observed value was 1.36 mmol g^{-1} in SP at an identical CLD. At the beginning of the SP, the more reactive bifunctional monomer forms compact nuclei, which bury the epoxy group of the monovinyl monomer (GMA), and thus are not favorably available for surface-related determination.

It was observed that copolymers prepared by FP and SP without a porogen have low pore volumes (H1–H20 and G1–G20; pore-volume data is not shown). Comparing the use of AIBN and BPO, BPO produced the larger pore volume in both sets. The maximum pore volume was found in G8 (CLD = 100 mol%; BPO initiator), namely, 0.20 $cm^3 g^{-1}$; in all other samples, the pore volumes were 0.03–0.20 $cm^3 g^{-1}$. SP at identical compositions did not have any porosity, and the pore volume and surface area were as little as 0.03–0.09 $cm^3 g^{-1}$ and 5–15 $cm^2 g^{-1}$, respectively. The macroporous morphology and formation of porous texture is dictated by the presence of a porogen, its type, and relative volume.[43] In the absence of a porogen, the pore volume that results from meso- and macropores is very low. The total porosity in these matrices was also very low and varied within 5–15% in both methodologies for both sets. At the front temperature, a larger number of free radicals are produced and simultaneous front propagation occurs. At higher initiator concentration, more free radicals are generated per unit time, thus lowering the internal pore volume by favoring intramolecular cyclization reactions and resulting in compact nonporous or less-porous nuclei.

We compared the HEMA–EGDM copolymers prepared by both FP and SP using EEA as the porogen, and the monomer/porogen ratio was varied (1:0.4 and 1:0.8, v/v; Table 3). More than a threefold increase in intruded pore volume was obtained in the porogenic system in FP. At a monomer/porogen ratio of 1:0.4 (v/v), the maximum pore volume was obtained with CLD at 400 mol% for both initiation systems (Figure 6). At a monomer/porogen ratio of 1:0.8 (v/v), a higher pore volume was obtained with AIBN. However, these data may not be exact as there was competition from bulk polymerization during the reaction. In general, BPO produced a stable front and higher pore volume. A representative SEM image of the porous structure is shown in Figure 7. Brunauer–Emmet–Teller (BET) surface-area measurement data also revealed moderate surface areas of polymers (30–95 $cm^2 g^{-1}$) produced by FP suitable for chromatographic applications. The maximum surface area was obtained at a monomer/porogen ratio of 1:0.8 (v/v) with CLDs of 200 and 400 mol% with AIBN and BPO, respectively. FP produced a narrow pore-size distribution and higher porosities (30–50%) in the matrix. Identical compositions using SP did not yield porosity as a result of the solvating nature of EEA and absence of phase separation. The network collapsed as it formed to yield a glassy amorphous gel-type resin on drying. Moreover, bead formation did not take place in SP with a monomer/porogen ratio of 1:0.8 (v/v) with a BPO concentration of 4 mol% and only an agglomerated mass was obtained. FP also proved to be better

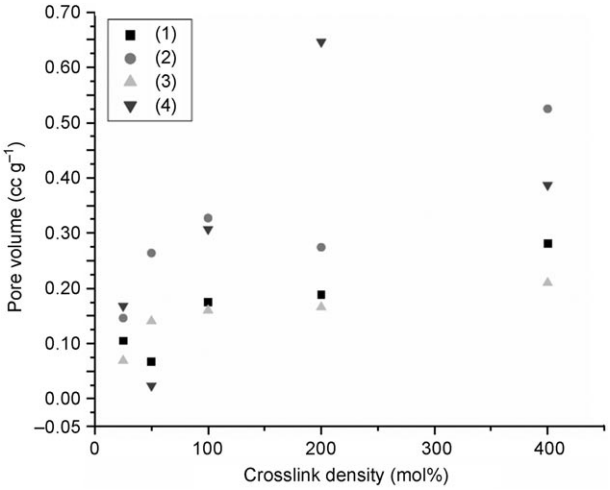

Figure 6. FP of the HEMA–EGDM system carried out using EEA as the porogen. 1) monomer/porogen: 1:0.4 (v/v) with 4 mol% BPO; 2) monomer/porogen: 1:0.8 (v/v) with 4 mol% BPO; 3) monomer/porogen: 1:0.4 (v/v) with 4 mol% AIBN; 4) monomer/porogen: 1:0.8 (v/v) with 4 mol% AIBN.

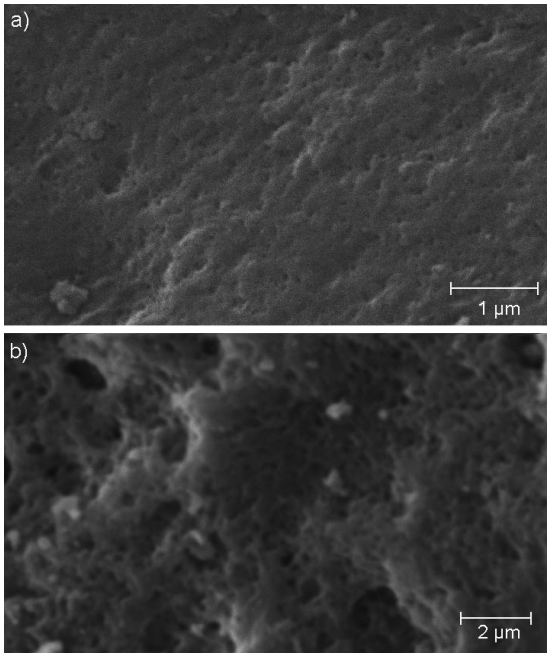

Figure 7. SEM images showing the porous structure of the polymer matrix: a) poly(GMA–EGDM) at 25 mol% CLD synthesized by using 4 mol% BPO; b) poly(HEMA–EGDM) at 2 mol% CLD synthesized by using a monomer/EEA ratio of 1:0.4 (v/v).

in terms of yield. SP produced lower yields of 40–60%, whereas the corresponding yields for FP were 65–95%, depending upon the reaction conditions (Table 4).

Pattern formation: Although the degree of crosslinking can be considered as a measure of bifurcation,[23,53] we did not observe the visible helical patterns in any of the systems. We observed that during the polymerization, along with gases,

monomer vapors also escape along the walls of the reactor tube. These vapors polymerize as they go in the upward direction and form a skin layer upon the already formed polymer. Therefore, it is highly probable that this skin layer is one of the reasons for the absence of helical patterns. When the patterns were observed carefully in sunlight, we could see weak helical patterns buried inside the skin layer that were not regular. When polymer rods (prepared without using a solvent) were broken along its axis, translucent and pale sections were observed. This behavior shows that hot spot(s) must be present and a pattern must have formed because of the spiral motion of the reaction zone. A similar experiment was reported by Manz et al.[23] for the FP of 1,6-hexanediol diacrylate. They showed the presence of a single head hot spot by slicing the gels and performing an MRI analysis of each slice followed by a computer-aided reconstruction. In our system, although the helical patterns were invisible, the traversal of a heat wave along the radical direction resulted in planar spatial patterns. The radial pitch of these patterns was very small and therefore were observable only by SEM analysis. Pujari et al. reported similar layered patterns in water-triggered FP.[54]

The detailed pattern formation (both planar and helical) is explained thus: The interplay of thermal diffusion and chemical kinetics during the FP reaction gives rise to pattern formation.[3] The pattern formation that occurs during the axial motion of the moving reaction interface is a complex phenomena. This behavior arises as a result of the occurrence of chemical instability when plane waves appear on both sides of the reaction interface that form a continuous motion. Furthermore, a difference in concentration gradients across the interface exists, thus indicating the presence of a narrow reaction zone that separates the gel and liquid phases.[40,55] Also, the planar reaction interface is at an uniform temperature, which is a front temperature that describes the steady state of the moving front. In addition, we note that the physicochemical phenomena of pattern formation is identified as the self-organization of wave motion in the vicinity of the spiral core. This spiral core forms around the center of the reactor tube along the radial axis. The spiral wave motion occurs along a radial coordinate,[56,57] along which the temperature or heat wave traverses and gives rise to a characteristic spatial wave form as a result of an interaction with the chemical kinetics. The moving reaction front descends at a constant speed of propagation, and the spatial pattern repeats itself. This behavior is still a planar motion of the moving reaction front and is termed an instability as it occurs at a critical point as a self-organizing phenomena. These spatial planar patterns are of two types: 1) a concentric ring pattern or 2) a characteristic pattern with an impulse followed with a smooth regular motion. Koga[57] reported conditions for the occurrence of such patterns for planar spiral motion, which can be easily extended to a case of a moving reaction interface. Under our experimental conditions, we did not observe concentric ring patterns; instead, we observed the second pattern. An SEM image shows the spatial patterns along the radial direction perpendicular to the axial motion (Figure 8a,b). In this case, the reaction is narrow and results in a planar front propagation. When the thermal diffusion spreads itself to the adjacent monomer and initiator mixture, the motion of the moving reaction interface becomes a nonplanar front propagation and still repeats itself as a steady characteristic spatial pattern. Again, these patterns are of two types: layered concentric rings and winding staircase patterns. The SEM image in Figure 8c shows the winding staircase pattern, whereas Figure 8d shows layered concentric rings. These layered patterns are formed during the front motion and are a self-organizing phenomenon.[58] We also observed some intermediate spatial patterns (not shown here) that are planar and nonplanar, but not a clearly identifiable pattern as discussed above. The mathematical analysis that explains the conditions for the pattern-formation phenomenon will be presented in a later communication.

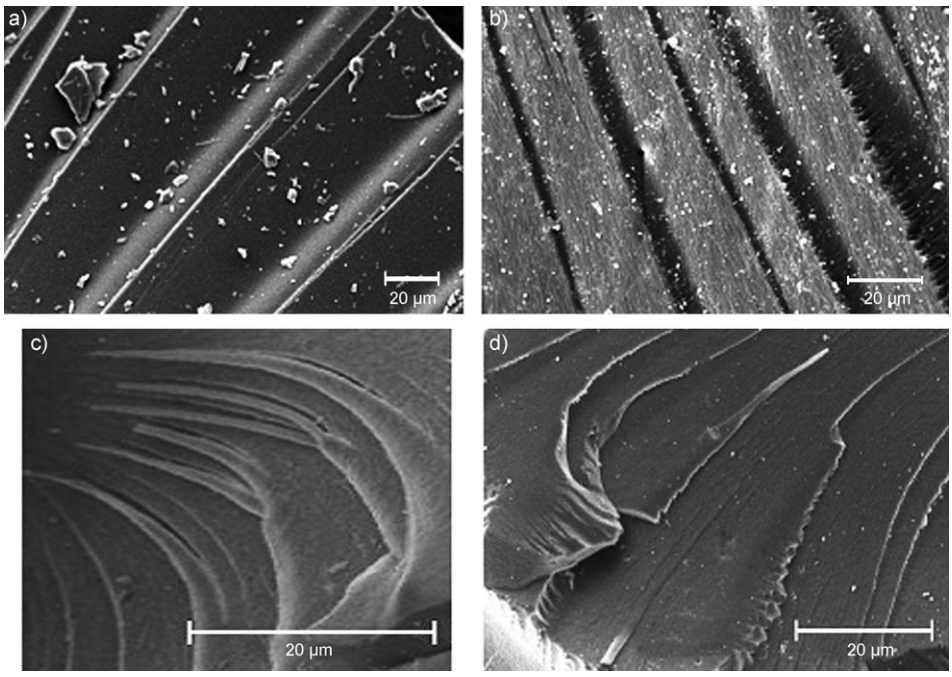

Figure 8. SEM images showing exotic patterns: Planner patterns of poly(HEMA–EGDM) at a) 25 mol% CLD, synthesized by using BPO (H16); b) 25 mol%, CLD synthesized by using 2 mol% AIBN (H11). Poly-(GMA–EGDM) synthesized at c) 50 mol% CLD, synthesized by 4 mol% AIBN (G17); d) 25 mol% CLD, synthesized by using a complex initiation system (AIBN+DCP).

In the presence of a solvent, the front temperature drops drastically. Therefore, we did not observe traces of spiral motion when we carried out the reactions in a porogen. Therefore, we may conclude that the occurrence of hot spots is controlled by temperature, and as the solvent controls the front temperature, the instabilities are absent in the system or the patterns might be very weak and unobservable.

Conclusion

A series of copolymers of HEMA/GMA and EGDM were synthesized by frontal polymerization. It was predominantly observed that the front initially propagates in the form of bubbles that try to escape along the walls of the reactor tube. The front stabilizes and propagates smoothly after the initial uneven movement. AIBN and BPO produced stable fronts, whereas the higher activation-energy initiator DCP could not sustain a front as a result of extensive heat loss. As a general observation, front velocity increased with increasing CLD (mol%). AIBN produced faster fronts than BPO, and a dual initiator system (AIBN + DCP) was found to be effective in stabilizing front propagation and resulted in higher yields. At lower initiator concentration, the front ceased when the reactions were carried out in the presence of solvents. Amongst several solvents evaluated, ethoxyethyl acetate (EEA) was found to sustain the front in the HEMA–EGDM system. All the reactions in the GMA–EGDM system were extinguished in the presence of a solvent. These reactions were sustainable only when diluents, such as silica gel, were added and at higher CLD. In the HEMA–EGDM system, bulk polymerization competed with pure FP at a higher monomer/solvent ratio of 1:0.8. In ascending polymerization, convective instabilities were observed and the front propagation was in the nonplanar mode. Interestingly, we could perform reactions in DMSO, which was otherwise not possible in descending polymerization.

The synthesized polymers were also compared with SP, as functionalized polymers are prepared by SP for chromatographic and enzyme-binding applications. When reactions were carried out without a solvent (porogen), pore volumes were lower and discontinuous. EEA was evaluated as a porogen for the first time, and it was observed that sufficient pore volume and specific surface area was produced. Pore volume and specific surface area in FP were found to be independent of the crosslinker but dependent on the type and volume of the solvent. At higher volumes of EEA, higher pore volumes were generated. Pore-size distribution in FP was also narrow and within 10–50 nm. In the presence of a porogen, the porosity was continuous. With identical compositions, SP could not produce porosity in the matrix as a result of the lack of incipient phase separation. Suspension polymerized beads were glassy and nonporous. Thus, FP was found to be superior over SP in terms of producing higher pore volume with or without a solvent, higher yields, and shorter reaction times.

The presence of exotic patterns is an important finding in this study. Polymers possessed spatial patterns along the radial direction, observable by SEM analysis. These patterns were of two basic types, namely, planar and nonplanar. The physicochemical understanding of the process is explained.

Experimental Section

Materials: GMA, HEMA, and EGD were obtained from Sartomer (USA) and used as received to prepare the copolymers. AIBN was obtained from SISCO (India) and recrystallized from methanol before use as an initiator. All the other reagents were used as received.

Polymerization: Thick-walled test tubes graduated in 1-mm intervals (12 (I.D.)$\times$125 mm) were used for the experiments. Polymerization was triggered with a soldering iron. The progress of the polymerizing front was monitored visually. The rate of the propagation of the front was timed with a stopwatch and reported as the velocity of the front (cm min^{-1}). A thermocouple (diameter = 0.125 mm; Hi-Tech Scientific, India), was inserted after the monomers and initiator (BPO, AIBN, DCP, or DCP/AIBN) were charged into the test tube. The temperature was measured relative to time with a programmable temperature controller (Hi-Tech Scientific, India). Monomer feed ratios and copolymer composition are indicated as CLD (mol%): the mole percent of the crosslinking divinyl monomer EGDM relative to the functional monovinyl monomer HEMA or GMA. The reactions were videotaped at 50–400 frames s^{-1} using a Red Lake Imaging, Motionpro model attached with AF micro Nikkor 105-mm lens charge-coupled device (CCD) camera. A few experiments were triggered by a heat source at the bottom (ascending FP).

Copolymers formed were ground using a blender, purified by washing several times with methanol and water, and dried in a vacuum oven at 50 °C for 36 h.

Suspension polymerization: The synthesis was conducted in a double-walled cylindrical reactor fitted with an eight bladed Ruston turbine stirrer and a nitrogen inlet. The continuous phase comprised of an aqueous solution of poly(*N*-vinyl-2-pyrrolidone) (PVP; 1%, w/w). The discontinuous organic phase consisted of GMA, the crosslinking divinyl monomer EGDM, and the polymerization initiator AIBN. The discontinuous organic phase was introduced into the aqueous phase, stirring was set at 300 rotations min^{-1}, and the temperature was maintained at 70 °C by circulating hot water. The reactant compositions were identical to those used in FP. The polymerization was continued for 3 h. The copolymer obtained in beaded form was separated by decantation, washed with water and methanol, and dried at room temperature under reduced pressure.

Both sets of copolymers, obtained from FP and SP, were sieved using Kumar test sieves (Mumbai, India) to obtain uniform particles of similar size (80–100 mesh), which were used for characterization.

Characterization: The surface epoxy/hydroxy functional groups of the copolymers were estimated titrimetrically.[10,11] Millimoles of epoxide/hydroxy per gram of polymer was estimated by end-group analysis.

The skeletal density d_b and the apparent density d_a of the polymers were measured by picnometry with mercury as the confining fluid. The copolymers were degassed in a picnometer and filled with mercury under vacuum at 25 °C. From the density measurements, the total porosity in the matrix was estimated from Equation (1).

$$\text{porosity}\ (\%) = (1-d_b/d_a) \times 100 \quad (1)$$

Mercury intrusion porosimetry (Quantachrome Corp., USA) was used to estimate pore volume, and the specific surface-area measurements, based on the single-point nitrogen adsorption method (more popularly known as the BET method), were conducted using a surface area analyzer (Quantachrome Corp., USA).

A scanning electron microscope (Phillips model XL 30) was used for morphological observation of the polymers. These polymers were cut

carefully from different parts of the column and mounted on stubs and sputter coated with gold to visualize the surface morphology.

Acknowledgements

The authors thank DST (New Delhi, India) for funding this investigation, A. Gorasia and Dr. V. V. Ranade for the CCD camera experiments, and the CSIR (New Delhi, India) for a research fellowship (N.S.P.).

[1] N. M. Chechilo, R. J. Khvilivitskii, N. S. Enikolopyan, *Dokl. Akad. Nauk SSSR* **1972**, *204*, 1180.
[2] J. A. Pojman, *J. Am. Chem. Soc.* **1991**, *113*, 6284.
[3] J. A. Pojman, V. M. Ilyasnenko, A. M. Khan, *J. Chem. Soc. Faraday Trans.* **1996**, *92*, 2825.
[4] J. A. Pojman, D. I. Fortenberry, V. M. Ilyashenko, *Int. J. Damage Mech. Int. J Self-Propag. High-Temp. Synth.* **1997**, *6*, 355.
[5] J. A. Pojman, J. Willis, D. V. Fortenberry, V. M. Ilyashenko, A. Khan, *Solvent-free synthesis by free-radical FP* (Eds.: T. E. Long, M. O. Hunt), *ACS Symposium series* 713, American Chemical Society: Washington, DC, **1998**, p. 140.
[6] A. M. Khan, J. A. Pojman, *Trends Polym. Sci.* **1996**, *4*, 253.
[7] S. Chen, J. Sui, L. Chen, J. A. Pojman, *J. Polym. Sci. A: Polym. Chem.* **2005**, *43*, 1670.
[8] Q. Z. Yan, X. T. Lu, W. F. Zhang, C. C. Ge, *Chem. Eur. J.* **2005**, *11*, 1609.
[9] Q. Yan, W. F. Zhang, G. D. Lu, X. T. Su, C. C. Ge, *Chem. Eur. J.* **2006**, *12*, 3303.
[10] N. S. Pujari, A. R. Vishwakarma, T. S. Pathak, S. A. Mule, S. Ponrathnam, *Polym. Int.* **2004**, *3*, 2045.
[11] N. S. Pujari, A. R. Vishwakarma, T. S. Pathak, A. M. Kotha, S. Ponrathnam, *Bull. Mater. Sci.* **2004**, *24*, 529.
[12] T. Hu, S. Chen, Y. Tian, J. A. Pojman, L. Chen, *J. Polym. Sci. A: Polym. Chem.* **2006**, *44*, 3018.
[13] A. Mariani, S. Bidali, S. Fiori, G. Malucelli, L. Ricco, *Macromol. Symp.* **2004**, *218*, 1.
[14] S. Vicini, A. Mariani, E. Princi, S. Bidali, S. Pincin, S. Fiori, E. Pedemonte, A. Brunetti, *Polym. Adv. Technol.* **2005**, *16*, 293.
[15] R. P. Washington, O. Steinbock, *Polym. News* **2003**, *28*, 303.
[16] I. P. Nagy, L. Sike, J. A. Pojman, *J. Am. Chem. Soc.* **1995**, *117*, 3611.
[17] J. Szalay, I. P. Nagy, I. Barkai, M. Zsuga, *Angew. Makromol. Chem.* **1996**, *236*, 97.
[18] R. P. Washington, O. Steinbock, *J. Am. Chem. Soc.* **2001**, *123*, 7933.
[19] S. Fiori, A. Mariani, S. Bidali, G. Malucelli, *e-Polymers* **2004**, *1*, 1.
[20] J. A. Pojman, W. Elcan, A. M. Khan, L. Mathias, *J. Polym. Sci. A: Polym. Chem.* **1997**, *35*, 227.
[21] G. Bowden, M. Garbey, V. M. Ilyashenko, J. A. Pojman, S. Solovyov, A. Taik, V. Volpert, *J. Phys. Chem. B* **1997**, *101*, 678.
[22] J. Masere, F. Stewart, T. Meehan, J. A. Pojman, *Chaos* **1999**, *9*, 315.
[23] B. Manz, J. Masere, J. A. Pojman, F. Volke, *J. Polym. Sci. A: Polym. Chem.* **2001**, *39*, 1075.
[24] B. Binici, D. L. Fortenberry, K. C. Leard, M. Molden, N. Olten, S. Popwell, J. A. Pojman, *J. Polym. Sci. A: Polym. Chem.* **2006**, *44*, 1387.
[25] B. N. Novozhilov, *Pure Appl. Chem.* **1992**, *64*, 955.
[26] K. G. Shkadinsky, B. I. Khaikin, A. G. Merzhanov, *Combust. Explos. Shock Waves (Engl. Transl.)* **1971**, *1*, 15.
[27] T. P. Ivleva, A. G. Merzhanov, K. G. Shkadinskii, *Dokl. Akad. Nauk Arm. SSR* **1980**, *239*, 1086.
[28] S. B. Margolis, *Metall. Trans. A* **1992**, *23*, 15.
[29] B. J. Matkowsky, G. Sivashinsky, *SIAM J. Appl. Math.* **1978**, *35*, 465.
[30] A. Bayliss, B. J. Matkowsky, *SIAM J. Appl. Math.* **1990**, *50*, 437.
[31] V. M. Shkiro, G. A. Nersisyan, *Combust. Explos. Shock Waves (Engl. Transl.)* **1978**, *14*, 121.
[32] V. P. Begishev, V. A. Volpert, S. P. Davtyan, A. Y. Malkin, *Dokl. Phys. Chem.* **1985**, *279*, 1075.
[33] J. A. Pojman, V. M. Ilyashenko, A. M. Khan, *Physica D* **1995**, *84*, 260.
[34] J. A. Pojman, J. Masere, E. Petretto, M. Rustici, D.-S. Huh, M. S. Kim, V. Volpert, *Chaos* **2002**, *12*, 56.
[35] V. M. Ilyashenko, J. A. Pojman, *Chaos* **1998**, *8*, 285.
[36] V. Volpert, V. L. Volpert, *Eur. J. Appl. Math.* **1994**, *5*, 201.
[37] V. Volpert, V. L. Volpert, J. A. Pojman, S. E. Solovyov, *Eur. J. Appl. Math.* **1996**, *7*, 303.
[38] S. E. Solovyov, V. M. Ilyashenko, J. A. Pojman, *Chaos* **1997**, *7*, 331.
[39] B. McCaughey, J. A. Pojman, C. Simmons, V. A. Volpert, *Chaos* **1998**, *8*, 520.
[40] V. A. Volpert, C. A. Spade, *Combust. Theory Modell.* **2001**, *5*, 21.
[41] S. R. Inamdar, N. S. Pujari, I. A. Karimi, S. Ponrathnam, R. K. Tayal, B. D. Kulkarni, *Chem. Eng. Sci.* **2007**, *62*, 1448.
[42] O. Okay, *Prog. Polym. Sci.* **2000**, *25*, 711.
[43] P. Hodge, D. C. Sherrington in *Syntheses and Separations Using Functional Polymers*, Wiley, New York **1989**.
[44] F. Svec, J. Hradil, J. Coupek, J. Kalal, *Angew. Makromol. Chem.* **1975**, *48*, 135.
[45] N. Ajzenberg, A. Ricard, *J. Appl. Polym. Sci.* **2001**, *80*, 1220.
[46] J. A. Pojman, R. Craven, A. Khan, W. West, *J. Phys. Chem.* **1992**, *96*, 7466.
[47] E. Marco, S. Cuartielles, J. A. PenÄa, J. Santamaria, *Thermochim. Acta* **2000**, *362*, 49.
[48] J. A. Pojman, J. Willis, D. Fortenberry, V. Ilyashenko, A. Khan, *J. Polym. Sci. A: Polym. Chem.* **1995**, *33*, 643.
[49] P. M. Goldfeder, V. A. Volpert, *Math. Problems in Engineering* **1999**, *5*, 139.
[50] B. McCaughey, J. A. Pojman, C. Simmons, V. A. Volpert, *Chaos* **1998**, *8*, 520.
[51] N. S. Pujari, A. R. Vishwakarma, M. K. Kelkar, S. Ponrathnam, *e-Polymers* **2004**, *49*, 1.
[52] J. A. Pojman, S. Popwell, D. Fortenberry, V. A. Volpert, V. A. Volpert, *ACS Symposium Series* (Eds.: J. A. Pojman, Q. Tran-Cong-Miyata), American Chemical Society, Washington, DC, **2003**, 869, p. 106.
[53] N. S. Pujari, S. R. Inamdar, S. Ponrathnam, B. D. Kulkarni, *Macromol. Rapid Commun.* **2007**, *28*, 109.
[54] L. K. Gross, V. A. Volpert, *Stud. Appl. Math.* **2003**, *110*, 351.
[55] J. M. Greenberg, *SIAM J. Appl. Math.* **1978**, *30*, 199.
[56] S. Koga, *Prog. Theor. Phys.* **1982**, *67*, 164.
[57] A. Winfree, *Scientific American*, **1974**, June, 84.

Received: October 5, 2006
Revised: December 18, 2006
Published online: April 20, 2007

